UiT The Arctic University of Norway

Faculty of Health Sciences

Molecular Modelling of PDE3A Catalytic Domain

Andrea B. Antobreh

Master Thesis in Pharmacy - May 2020

UiT The Arctic University of Norway

Acknowledgements

This study was conducted at the Department of Medical Biology, Faculty of Health Sciences at UIT - The arctic university of Norway, between August 2019 and May 2020.

My experience of being a graduate research student has been highly educational. Throughout the process, I have dealt with relentless amount of challenges, and I have a sense of mastery as a result. The accomplishment of this work would not have been possible without my mentor and elder sister Gloria T. Antobreh Nketiah, whom I look up to daily. I sincerely thank her for her dedication, motivation and time throughout this process.

Also, I would like to thank my supervisors Aina Ravna and Erik Dietrichs, for introducing me to the world of homology modelling. I am grateful for their patience and guidance.

I also want to thank my fellow student Silje Mork who has always been my closest friend and interlocutor throughout the master's program. These years would not have been the same without you at my side.

Lastly, I want to show gratitude to my family for cheering me on and remembering me in prayers. I am eternally grateful for all the love and support I have received.

Tromsø May 2020

Andrea Barnie Antobreh

III

Abstract

Recent studies have highlighted the clinical benefits of regulating phosphodiesterase-3 enzymes. Inhibition of PDE3A has proven to aid in preventing and treating cardiovascular-related disorders and platelet dysfunction. Hypothermia is a condition that can cause cardiac arrest. However, there are no suitable inotropic drugs that are effective for use under hypothermic conditions. Being able to understand the properties and function of the PDE3A enzyme is therefore essential to the development of new drug inhibitors with exceeding potency. The challenge remains unresolved due to the scarcity of PDE3A crystal structure information.

In this study, three models of the PDE3A enzyme were created based on homology modelling. The aim of creating homology models of the PDE3A enzyme was to visualize and gather further structural information for future studies related to drug development. The models were constructed by using known 3D structures of evolutionarily related proteins. The PDB IDs of the three chosen templates were 1SO2, 1TAZ and 4NPV. The quality of the models was evaluated using PROCHECK and ERRAT.

The three constructed models were all of high quality and fitted well to their corresponding templates. However, the 1SO2-based model proved to be the most reliable and therefore suitable for virtual ligand screening procedure to identify potential binding compounds that can be used as PDE3A inhibitors. The overview of the active site interactions of the models revealed that residues Y751, T844, D950, F972, Q975 and F1004 are highly conserved and presumably essential for enzymatic activity and ligand binding. The structural information of the PDE3A models is a significant asset for the development of PDE3A drug inhibitors that are suitable for use under hypothermic conditions.

Table of Contents

List of Tables

List of Figures

Abbreviations

3D	Three-dimentional
5´AMP	Adenosine 5´-monophosphate
ADRB1	Beta-1-adrenergic receptor
BLAST	Basic Local Alignment Search Tool
cAMP	Cyclic adenosine monophosphate
cGMP	Cyclic guanosine monophosphate
CN	Cyclic nucleotide
COPD	Chronic obstructive pulmonary disease
C-terminus	Carboxyl-terminus
ICM	Internal Coordinates Mechanics
Kcat	Turnover number
Kd	Dissociation constant
Ki	The inhibitor constant
Km	The Michaelis-Menten constant
NO	Nitric oxide
N-terminus	Amino-terminus
PDB	Protein Data Bank
PDB ID	Protein Data Bank code
PDE	Phosphodiesterase
PKA	Protein Kinase A
RBS	Rigid body superposition
RMSD	Root-mean-square deviation
TM	Transmembrane

1 Introduction

1.1 Context of the study

The enzymatic activity of the phosphodiesterase 3 (PDE) enzymes has an important role in cardiac function through its effect in hydrolysing cyclic nucleotides (CN). The disintegration of the CN, cyclic adenosine monophosphate (cAMP), is a crucial step in the signalling pathway that mediates contraction of the heart the muscle. cAMP is a secondary signalling transmitter that exists in multiple places in the body (1). The degradation of the CNs is ascribed by PDEs. The subfamily of PDE enzymes such as PDE3 is an important group of enzymes, frequently found in the heart and smooth muscles (2). Drug inhibitors that act as targets for these enzymes are thought to increase cardiac inotropy and smooth muscle relaxation, which could improve cardiovascular function. Recent studies have proved that the use of PDE3 inhibitors, such as milrinone and levosimendan, ameliorates cardiac function during hypothermia and rewarming of hypothermic patients (3-5).

Temperature management during and after cardiac surgery can have advantageous neuroprotective effects on both intermediate and long-term outcome. During the temperature procedure, where the heart is arrested, patients often receive pharmacological treatment (6). In addition, accidental hypothermia can lead to complications of the heart, causing cardiac arrest and reduced circulation. Though controlled hypothermia and rewarming are sometimes necessary for best clinical outcome during surgery, the treatment of accidental hypothermia is more complicated and often associated with high mortality (7). In hypothermic conditions, the intracellular pathways modulating CN levels are altered. The major setback under these conditions often occurs during rewarming, causing victims to experience hypothermia induced cardiac dysfunction (5, 8, 9). Thus, adrenaline is frequently used to increase heart rate and contractility in case of cardiac dysfunction. The result is mediated by adrenalin activating beta-1-adrenergic receptors (ADRB1), which in turn increase the cAMP levels in cardiac myocytes. Consequently, the heart contracts after a series of phosphorylation of kinase enzymes. Unfortunately, adrenaline has been found to have reduced effect when used during hypothermic rewarming to 30 ^{o}C due to potential cardiotoxic side-effects (9, 10). There remains few pharmaceutical alternatives and treatment recommendations (9). Opportunely, further studies indicate that alternative routes that prevent the breakdown of cAMP may be a better alternative for treatment. PDE3 inhibitor milrinone used after rewarming from 15°C provided a stroke

volume and cardiac output within baseline values in treated animals (3). However, existing PDE3 drug inhibitors are designed for normothermic patients. Therefore, modelling of new PDE3 inhibiting drugs, specialized to be used under hypothermic conditions may provide a drastic improvement in the clinical outcome of this patient group.

1.2 Signalling pathway of cyclic nucleotides in the heart

The adenyl and guanine cyclase pathways are controlled by G protein-coupled receptor-triggered signalling cascade (1). These CNs are synthesized by the stimulation of

G-coupled protein receptors which, are positioned in the cellular transmembrane (TM) of myocytes. The CNs cAMP and cGMP are secondary signalling molecules that are activated by the stimulation of adrenergic receptors. The ADRB1 subgroup is most abundant in the heart (11), and therefore will be mainly discussed in this thesis.

The activation of the ADRB1 in the cardiac muscle leads to an increase of cAMP. In turn, cAMP activates protein kinase A (PKA). This enzyme is responsible for the phosphorylation of various proteins, which leads to a cascade of reactions resulting in the increased influx of intracellular calcium (L-type calcium channels). In turn, the activated calcium channels mediate calcium levels in the sarcoplasmic reticulum and contribute to cardiac contractility. There is also an increase in heart rate and smooth muscle relaxation as a result (12). The concentration of cAMP levels in the body is regulated by the PDE enzymes, which hydrolyse cAMP to Adenosine-5´-monophosphate (5´AMP) (13). PDE enzymes break down cAMP and thus inactivates the reaction cascade.

1.3 Phosphodiesterase enzyme family

PDEs are enzymes that hydrolyse and therefore break phosphodiester bonds. These enzymes play a role in regulation and signalling involving the adenyl and guanine cyclase system. In all, there are 21 genes that encode for the human PDE3 enzymes. There are 11 known families of PDE enzymes (2). The structural variations between these families enable the enzymes to have a widespread of signalling outcome. Although the enzymes reside in assorted parts of the body, the differences in structure between families and subfamilies of PDEs, generate substrate-specific hydroxylation. PDE enzymes have a characteristic property of disintegrating and eliminating the intracellular concentration of cAMP and cGMP. PDE1, PDE2, PDE3, PDE10 and PDE11 hydrolyse both cAMP and cyclic guanosine monophosphate (cGMP), while PDE 4, PDE7 and PDE8 are more specific to hydrolysing cAMP. PDE5, -6 and - 9 are cGMP specific

(14). cAMP and cGMP occur through a widespread of places in the body. They are important secondary signals that mediate functions involving the heart, blood vessels, hormones and smooth muscle, for example. Being able to inhibit and thus alter the functions of PDE enzymes is, therefore of great clinical relevance.

1.3.1 Phosphodiesterase inhibitors

In order to make a viable inhibitor drug, one must have a good understanding of the interactions necessary to form a stable binding complex between the drug and its target molecule (15). CNs are widely distributed in the body and have many functions depending on their location. Nevertheless, inhibiting different PDE enzymes will produce different effects depending on where in the body the inhibition takes place (2). Thus, inhibitors of PDE enzymes must be specific to their target proteins to increase affinity and decrease side effects.

Examples of drugs that are used to inhibit PDE enzymes are rolipram and milrinone, which are used to treat asthma and heart failure, and are selective for PDE4 and PDE3, respectively. Milrinone has proven to be a promising drug supporting hemodynamic function during hypothermia and rewarming (3). Finally, PDE5 inhibitor drug sildenafil, or otherwise marketed as Viagra, is used to treat erectile dysfunction. Most selective inhibitors are being developed mainly to treat cardiovascular and respiratory diseases (16). Table 1 shows an overview of PDE inhibitors that are frequently used and their mechanism of action (17).

Table 1. *Some inhibitors of PDE enzymes and their mechanism of action.*

	Active ingredient	Indication	Effect

Nonspecific PDE inhibitors (inhibitors of PDE3, -4 and -5)	• Theophylline	• Chronic obstructive pulmonary disease (COPD)
		• Asthma
			• Hydrolysis of cAMP is decreased causing increased cAMP levels:
			  o Inhibits proinflammatory mediators
			  o Deceleration of fibrotic changes in lung
			  o Relaxation of bronchial musculature

PDE5 inhibitors	• Sildenafil (Viagra)
	• Tadalafil
		• Erectile dysfunction
		• Pulmonary hypertension
			• Breakdown of cGMP is decreased causing increased cGMP levels:
			  o Smooth muscle relaxation in reaction to nitric oxide (NO) activation.
			  o Pulmonary vasodilatation
			  o Penile smooth muscle relaxation

PDE4 inhibitors	• Roflumilast	• Severe COPD	• PDE4 inhibition causes increased cAMP levels in neutrophils, granulocytes and bronchial epithelium:
			  o Inhibition of proinflammatory mediators
			  o Deceleration of fibrotic changes in the lung
			  o Relaxation of bronchial musculature

PDE3 inhibitors	• Milrinone
	• Amrinone
	• Cilostazol
	• Dipyridamole
		• Acute treatment of decompensated cardiac failure with cardiogenic shock.
		• Intermittent vascular claudication
		• Antiplatelet; Angina/TIA/Stroke prevention
		• Prevention of coronary stent restenosis
			• PDE3 inhibition causes increased cAMP in myocardium, peripheral vessels and platelets:
			  o Heart contractility increases
			  o Smooth muscle relaxation
			  o Inhibition of platelet aggregation

1.3.2 Common structural properties of PDE enzymes

Each PDE enzyme contains a catalytic domain, a long amino-terminus (N-terminus) that may contain one or more structured domains and an unstructured carboxyl- terminus (C-terminus) (2, 18). The function of each region varies between the different PDE families. The primary sequences of the PDE enzymes all have a common catalytic core. This core is responsible for enzymatic activity and is therefore most conserved (18). In a study featuring the structure and ligand interactions of PDEs, it was shown that most PDE enzymes that have been crystallized, tend to bind to the substrate binding pocket of the PDE catalytic domain (2). The catalytic domain consists of up to 16 helices and 16 loops that fold to form a substrate binding pocket (18).The phylogenetic tree of the human PDE families reveals that the PDE3A enzyme family is closely related to PDE3B and PDE1B (Figure 1) (2).
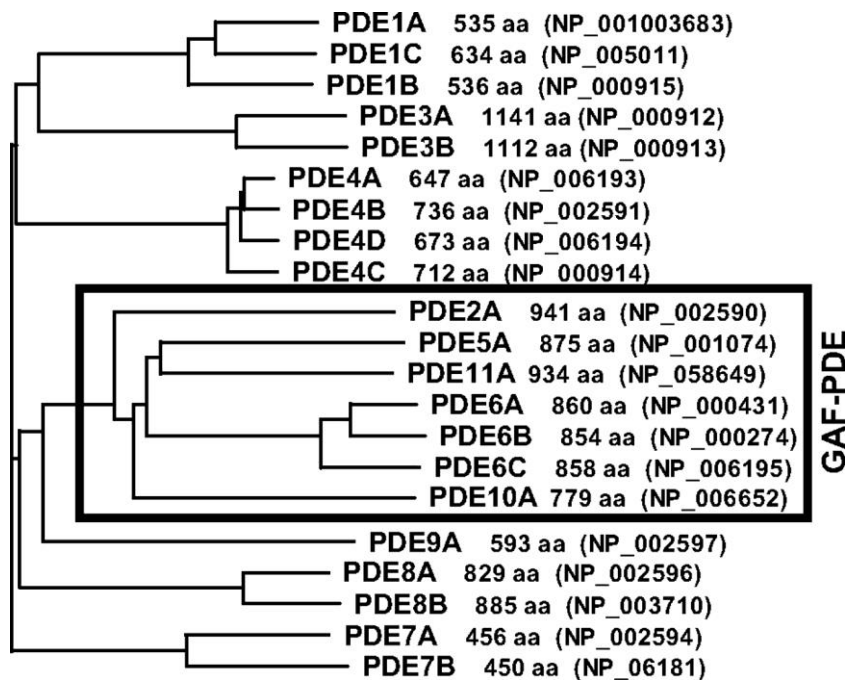
Figure 1. *Phylogenetic tree of human PDE families 1 to 7. (2).*

1.4 Phosphodiesterase 3 subfamilies

This enzyme subfamily is often called cGMP inhibited cAMP PDE enzymes because they hydrolyse both cAMP and cGMP, although they have a higher affinity to cAMP (2). The PDE3 family can be divided into two main groups: PDE3A and PDE3B. There is a 44 amino acid long insert located within the catalytic core that is unique for the PDE3 isomers (18, 19). This insert is supposedly positioned between second histidine and the glutamate of the first motif (AA position 773-816) (18, 20, 21). The active site is known to lay between amino acids 679 and 1141 (21). In the heart, PDE3A is most common (22), however, to our knowledge there is no crystallized structure of the PDE3A enzyme family at the time of writing this thesis. Nevertheless, there is a crystal structure of PDE3B (PDB ID: 1SO2) published in the protein data bank (PDB) database. In order to increase the accessibility and effectiveness of a potential drug that works on the heart, it is appropriate to use the most abundant subgroup of PDE3 as the target molecule. Therefore, the focus of discovering a new inotropic drug is directed on PDE3A subgroup. Nevertheless, the published PDE3B model will act as a major asset in making a homology model of PDE3A enzyme for this thesis.

1.4.1 Structure of PDE 3A

PDE3A enzyme consists of 1141 amino acids (23). The amino acid sequence of this enzyme is the longest of all compared to the other crystalized and modelled PDE enzymes in the family (see Figure 1). Similar to the other PDE enzymes, the PDE3A also has a catalytic core closer to the C-terminal of the protein (18). The TM domain of the enzyme consists of 6 alpha helices and binds the PDE3 to the endoplasmic reticulum and other membrane rich regions of the cell (see Figure 2). The amino acid TM areas of a protein are normally highly conserved and are bound together by loops that are less conserved (2). According to the visualized figure of PDE3A in Figure 2, the N-terminal and C-terminal of the enzyme are extracellular, along with the loops between TM helix 2 and 3, and TM helix 4 and 5. The intracellular region consists of the largest loop between TM helix 1 and TM helix 2 along with the rest of the remaining loops. The N-terminal containing the hydrophobic TM loops is responsible for the phosphorylation and activation of the enzyme by PKA and PKB (14, 19, 24). The catalytic domain of PDE3 is adjacent to the C-terminal of the protein and is responsible of the hydrolysis of the CN. The reaction occurs in the substrate-binding pocket, catalysed by divalent metal cations that occupy

adjacent metal-binding regions (23). This is normally a zinc ion site 1, while site 2 prefers magnesium and/or manganese ions.
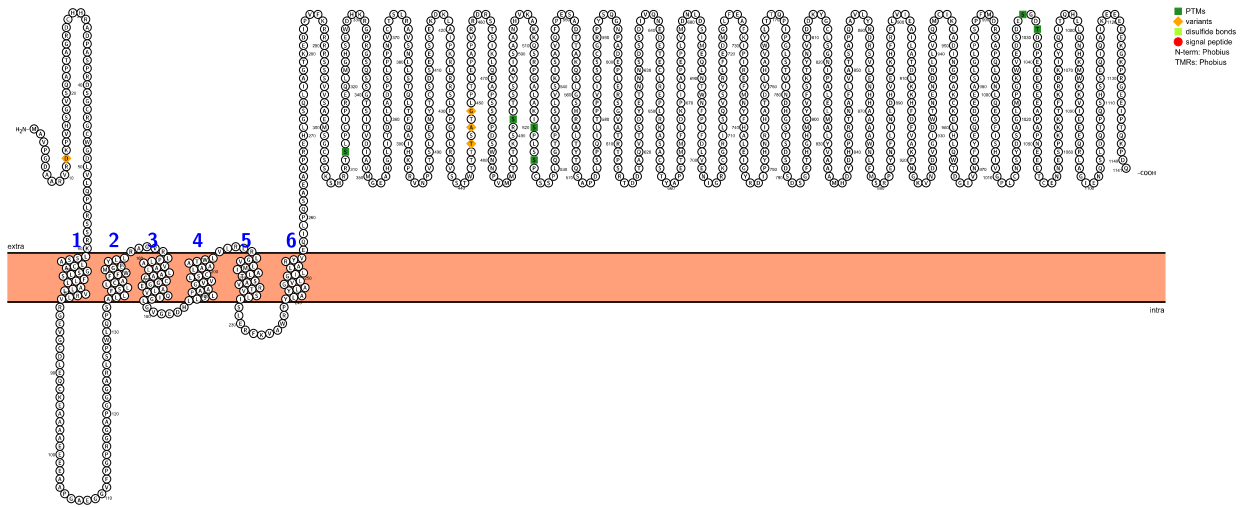
Figure 2. *Visualization of the PDE3 enzyme (UniProt protein accession id: PDE3A_HUMAN) generated from protter (http://wlab.ethz.ch/protter/start/). There are 6 alfa helices in the TM domain.*

1.4.2   Ligand binding site

Ligand binding occurs in the catalytic domain of the enzyme. The binding site of the enzyme is also where the hydrolysis of cAMP (and cGMP) occurs. This area appears to be composed of the amino acids from D680 to D1105. In this area, it is also common to have 44 amino acid inserts that start from P773 to C816 (18). There is a total of 16 alpha helices that create three domains in the catalytic region, which is located in a dim pocket between the three subdomains (25). Previous mutagenesis studies have shown that the conserved residues Y751, D950 and F1004 are responsible for binding both substrate and inhibitor (26).

1.4.3   PDE3 inhibitors; mechanism of action

PDE3A is a dual enzyme which is specific for both cAMP and cGMP (14). By hydrolysing cAMP in the heart, the signal that is responsible for maintaining heart contractions is reduced. A PDE3 inhibitor acts as a competitive substrate for the PDE enzyme. When the inhibitor is bound to the PDE3 enzyme, the enzyme will be occupied and therefore unable to hydrolyse cAMP as a result. This will cause an increase in the concentration of cAMP in myocytes. Increased inotropic effect on the heart is a consequence, which is not reduced to the same extent as adrenergic receptor stimulation during hypothermic conditions (3, 27).

1.5 Drug-enzyme interactions and affinity

Interactions among enzyme and substrate, and the strength of the intermolecular forces between them, will affect ligand affinity and specificity. To make a PDE3A specific inhibitor that can compete with the natural occurring substrates, it is crucial that the inhibitor has a stronger affinity for the enzyme, and reasonable binding specificity. Therefore, it is important to have an overview of the drug-enzyme interactions and affinity before conducting a competitive inhibitor. Binding stability can also be affected by nearby residues and hydrophilicity in the environment where the bonding takes place. Strong bonds are often stable and require much energy to break (28). Covalent bonds are the strongest. There are no covalent bonds occurring between the PDE3 enzymes and substrate. The only interactions that occur between the enzyme and substrate are electrostatic ones (29). Interactions with low refractive energy are easier to manipulate and break (28). High specificity and affinity between an enzyme and its substrate are a result of the additive effects of multiple interactions between the two molecules. In general, binding affinity is additive, and several strong interactions between the enzyme and substrate will be desirable for the most stable complex. Nevertheless, strong bonds that are stable can also cause the enzyme to become more rigid. An enzyme locked in a specific conformation may be less effective because this might cause reduced flexibility when making room for diverse ligand binding (28, 29). Preferably the binding affinity interactions should not be at the expense of reduced turnover rate.

1.5.1 Electrostatic interactions

- Ionic interactions: Ionic bonds are non-covalent interactions between two ionized residues with opposite charges. Amino acids can have a negative, positive and neutral charge in physiological pH. The possibility of ionic binding occurs when the components are charged. Positively charged amino acids act as hydrogen bond donors and the negatively charged amino acids are hydrogen bond acceptors. The amino acids that are positively charged in physiological pH are arginine (R), lysine (K) and histidine (H), while those that are negatively charged are aspartic acid (D) and glutamic acid (G). This interaction is considerably weaker than the covalent bonds but is the driving factor for ligand binding and affinity. These types of interactions, initially described by coulomb`s law, is water and pH dependent. The interaction has two components: a hydrogen bond and an electrostatic interaction. Coulomb's law describes the

relationship between force, charge and distance, indicating that the interaction depends on the charge of the atoms on opposite sides; Z_A and Z_B and the distance, as well as the dielectric constant, E_0 (see Figure 3).

$$\text{Coulomb's law : } \Delta E = K \frac{Z_A Z_B}{r_{AB}^2}$$
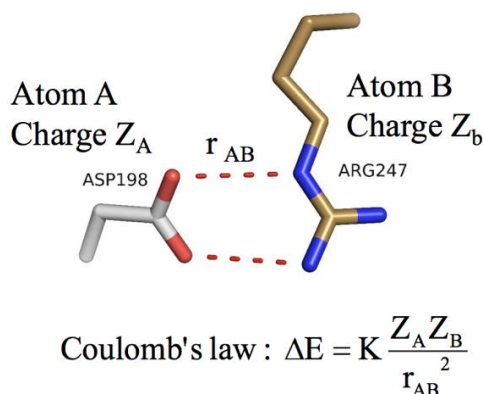
Figure 3. *Representation of coulomb`s law.*

- <u>Ion-dipole interactions</u>: The ion-dipole interaction is a result of an interaction between a partially charged atom and a neighbouring ion with an opposite charge. These kinds of interactions are also dependent on distance, pH and environmental hydrophobicity.

- <u>Dipole-dipole interactions</u>: Dipole-Dipole interactions occur between molecules that have permanent dipoles. These molecules are also referred to as polar molecules.

- <u>Hydrogen bonds</u>: These are interactions that occur between two electronegative atoms, e.g. Nitrogen or Oxygen. The electronegative atoms, in this case, are interacting with the same H-atom. The H-atom usually is covalently attached to the donor and interacts electrostatically with the acceptor. Hydrogen bonds are interactions between two electronegative atoms and one proton.
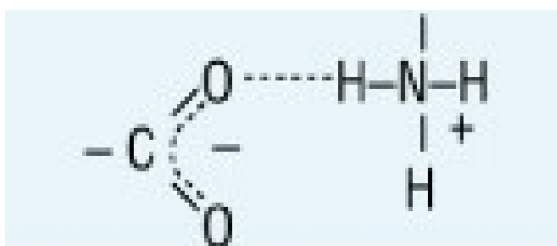
Figure 4. *The electrostatic interactions between hydrogen bond donors and hydrogen bond acceptors.*

Figure 4 is a visualization of hydrogen bond interactions between negatively and positively charged molecules. The electronegative oxygen atom draws on the partially positive hydrogen protons. Even though these interactions are typically strong, the

9

molecule shares its interactions with water molecules in the area, making hydrogen bonds affected by the hydrophilicity in the environment. Hydrogen bonds are thus stronger in an environment with less water molecules such as in the core of a protein active site.

- Van der Waals interactions: these interactions are "electrostatic" interactions between uncharged groups. The effect is greatest with groups that are most polarizable; usually methyl groups and methylene groups of hydrophobic side chains such as valine (V) and leucine (L).

1.5.2 Kinetic parameters that affect binding affinity

- Dissociation constant (Kd): The affinity between a ligand and a protein is often correlated with the bonding strength. A ligand that has a high enzyme affinity is more attracted to its target molecule and binds effortlessly. This can be explained as the Kd. A low dissociation constant means that a ligand is strongly bound to its receptor and a low concentration is needed to occupy the target molecule.

- Turnover number (Kcat): Kcat is used as a parameter to assess how many substrate molecules that are being "turned over" by the enzyme per second. High Kcat is equivalent to an effective enzyme.

- The Michaelis-Menten constant (Km): Km is a description of concentration and rate of reaction. It is a measure for affinity because it is descriptive of the maximum rate of the reaction occurring and the substrate concentration that is required to reach Vmax (maximum reaction rate). Low Km indicates that lower concentrations of substrate is required to reach maximum rate of reaction and is thus associated with high affinity.

- The inhibitor constant (Ki): Similar to Km, Ki is the concentration which is needed to reach the maximum reaction rate. Ki is therefore a measure of how potent inhibitors are. Low Ki means low concentration needed to reach maximum reaction rate and therefore high inhibitor potency.

- Km/Kcat: The relationship between Km and Kcat explains the catalytic efficiency of an enzyme. While a low Km is an indicator of high affinity, high Kcat is equivalent to effectiveness. The ratio that results in a low Km/Kcat is therefore preferable for the most effective and potent drug- enzyme reaction.

1.6 Homology modelling

Homology modelling is a tool that is used to synthetize a model of proteins for which the 3D structure does not exist. This technique is based on the observation that evolutionary related proteins share similar sequences and protein structures. Homology modelling provides easy access to structural and conformational properties of a protein without depending on advanced and time-consuming methods such as X-ray crystallography and NMR to conduct a 3D structure. This method requires a known structure to be used as a template(30). While PDE3B and PDE1 subtype has been crystalized several times, the crystal structure of PDE3A remains unknown. The function and physiological properties of a protein is dependent on its 3D structure. The model visualization of the protein structure of the PDE3A enzymes will help determine and understand its stability, active site and protein-ligand interactions that provide enzymatic affinity and efficiency.

Because of sequential similarities, the previously crystalized protein variants and their models can be used as a template to make a model of the PDE3 enzyme. Information about the protein structure and its active site is crucial for understanding and synthetizing new potential inhibitors. There are multiple steps to execute homology modelling as shown in Figure 5, the main steps include:

- Searching for a suitable template
- Aligning and comparing target and template sequence
- Building a homology model
- Refining and validating the models.
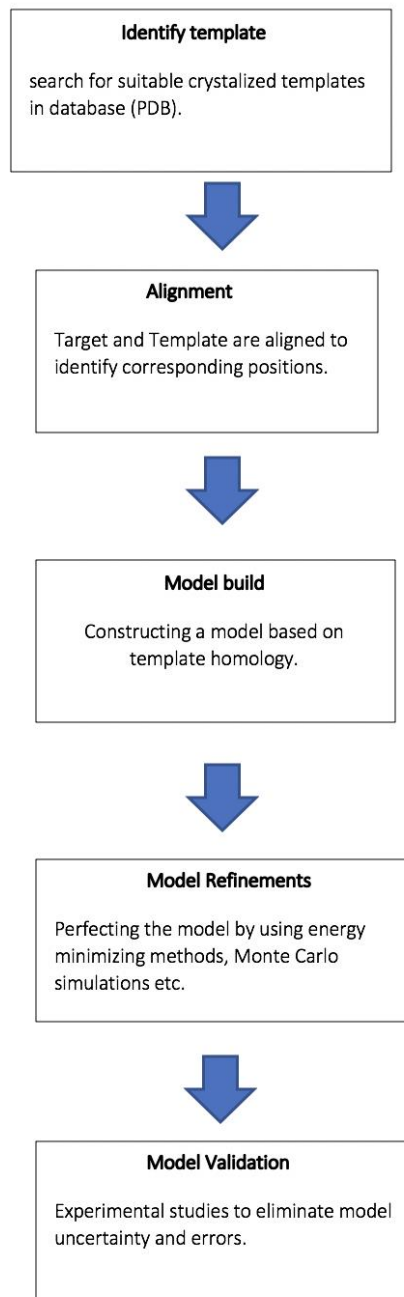
Figure 5. Flow Chart indicating important steps of homology modelling.

1.6.1 Template selection

When choosing a template to perform homology modelling, it is important to choose one that will provide the most reliable results. It is common to use databases such as PDB to find a suitable template. The PDB database, provides an overview of all crystallized proteins that have been published. To create a homology model, a crystallized structure which preferably has as much sequence similarity as possible with the target protein is chosen as a modelling template

(30). Although modelling might yield results that deviate and might contain errors, it is a much easier and time-saving approach. Though a homology model might be less reliable than a 3D crystal structure, the outcoming model quality can be influenced by how contemplative the template selecting step is. The PDB database accommodates published 3D structures of proteins in an active or inactive form. These are also often bound to ligands that they have been crystalized with. One should therefore carefully appraise when choosing a suitable template for a homology model. The preferred template should depend on the preferred form of the target molecule. The most comparable template choice must be the structure that is most similar to the target protein. High sequence identity and similar binding configuration must be prioritizing factors when choosing a template to construct a model of high quality. The crystal structures have also been made using various methods and equipment. Because of this, the templates can have varying quality. The chosen template structure must have a high resolution. The template selection step also influences model reliability. Fortunately, there are aids to help investigate these factors after conducting a model. Template selection is often simplified with database tools such as the basic local alignment search tool (BLAST) (31) which is also available through PDB and internal coordinate mechanics (ICM) software (32).

1.6.2 Sequence-structure alignment

Before creating a model, it is important that the target sequences are aligned to the template of choice (30). The goal of this is to determine sequence identity percent and thus corresponding positions in the target and template. During this step, one can also adjust the alignment to get the best result. The rule of thumb is that a sequence identity of over 50% is expected to provide a reliable model. A sequence identity between 30-50% provides satisfactory results, though potential errors should be expected and considered to make a reputable model. Optimization is especially required for the areas in a loop conformation. The target and template might have vastly different structures when the sequence identity is below 30%. Therefore, a sequence identity under 30% is known as the twilight zone. This means that one can expect unclear and inaccurate results due to a lack of sequence similarity between the target and the template (28). To increase the percent identity, insertions and deletions must be recognized. Insertions include inserting relevant amino acids to the sequence, while deletion is deleting or replacing irrelevant residues in the target. The goal is to adjust sequence alignment to conduct a reliable alignment and increase sequence identity before building a model.

1.6.3   Model build

After aligning the template and target sequence, a homology model can be conducted. Model building involves constructing the core areas of a protein based on the template (30). Molsoft ICM-PRO is one of the widely used homology modelling programs for creating models. Homology modelling using ICM-PRO is based on the Internal Coordinate Mechanics. Using this program structure prediction of protein sequences and drug design is possible (33). Molsoft ICM-PRO is available at http://www.molsoft.com/about.html. Model building consists of multiple steps involving modelling of core TM domains, loop modelling and side chain optimization using rigid body superposition (RBS) (30).

1.6.4   Model refinement

After building, a model refinement is implemented in order to ensure energy minimizations. This involves refining the uncertain parts of the model. Residues that are in unlikely conformations must be re-evaluated. Large side chains that are adjacent can cause steric clashes. This makes the model unreliable as sidechain residues naturally will sought the most stable conformation. A realistic model is therefore a model that has a low and stable calculated energy of the sidechain residues.

1.6.5   Model evaluation

After model building and refinement, an evaluation is done to ensure the validity of the model. Despite high sequence identity and low energy, errors in models are often unavoidable. Most prevalent errors are often associated with side chain packing, uncertain and unaligned loop regions, and unbeneficial adjustments that have been made. Experimental studies are therefore necessary for model validation. The stereochemical quality of the model is often analysed using easily accessible structure analysis servers such as PROCHECK and WHATCHECK (30).

2 Aim

Understanding the molecular mechanisms of a target molecule is crucial for developing corresponding active and effective ligands. To our knowledge, there are no published crystal structures of the PDE3A enzyme at the time of this study. Constructing a structure of the PDE3A enzyme is the first step to creating drug inhibitors that can be used to treat hypothermic patients. Therefore, the aim of this study is to conduct three homology models of the uncrystallised PDE3A enzyme, using existing crystalized structures of PDE enzyme family members as a template. Subsequently, the models will be evaluated to determine model accuracy and stability. Furthermore, the objective is to locate the active site residues that are necessary for inhibitor binding affinity and thus enzymatic activity. Information about the model may provide an overview of structural and functional information that is required for optimal enzymatic efficacy. This information is largely relevant for future development of PDE3A drug inhibitors for hypothermic patients.

3 Methods

3.1 ICM Homology modelling

The PDE3A enzyme was not crystalized at the time of this study. Therefore, a homology model was built based on homologous proteins. The steps consisted of finding suitable templates, alignment of template and query sequence and model building using ICM-PRO. Finally, the models were refined, evaluated and examined.

3.1.1 Template search

The query sequence of the human PDE3A enzyme was extracted from the UniProt database (www.uniprot.org). The UniProt accession number Q14432 was used when searching for possible templates. BLAST was used to find crystalized 3D structures of homologous proteins with high sequence similarity. The protein-protein BLAST search was conducted directly through the ICM program. The search was limited to find only crystalized 3D structures published in the PDB (https://www.rcsb.org/). As a result, a list of structures that could be potential templates were presented. The structures with the highest sequence identity and similarity to the PDE3A human enzyme were presented at the top of the list provided by the BLAST search. The top three crystal structures on the list were chosen as templates for making a homology model of the PDE3A enzyme. The structures chosen had the PDB ID´s 1SO2, 1TAZ and 4NPV. The query sequence of the human PDE3A and the 1SO2, 1TAZ, 4NPV sequences share 84%, 47% and 47% sequence similarity, respectively. The corresponding sequence identity between these structures are 69%, 32% and 32%.

The crystal structures of the templates were obtained, and the template sequences were extracted from the structures and downloaded directly into ICM.

Table 2. *Top 3 results of the BLAST search. These structures were chosen as templates for homology modeling for PDE3A enzyme.*

PDB ID	Structure Title	Sequence similarity (%)	Sequence identity (%)	Resolution (Å)	Primary Citation Author	PubMed ID
1SO2	Catalytic domain of human phosphodiesterase 3B in complex with a dihydropyridine inhibitor	84	69	2,4	Scapin, G., Patel, S.B., Chung, C., Varnerin, J.P., Edmondson, S.D., Mastracchio, A., Parmee, E.R., Singh, S.B., Becker, J.W., Van Der Ploeg, L.H., Tota, M.R.	15147193
1TAZ	Catalytic Domain of Human Phosphodiesterase 1B	47	34	1,77	Zhang, K.Y.J., Card, G.L., Suzuki, Y., Artis, D.R., Fong, D., Gillette, S., Hsieh, D., Neiman, J., West, B.L., Zhang, C., Milburn, M.V., Kim, S.-H., Schlessinger, J., Bollag, G.	15260978
4NPV	Crystal structure of human PDE1B bound to inhibitor 7A (6,7,8-trimethoxy-N-(pentan-3-yl) quinazolin-4-amine)	47	34	2,4	Humphrey, J.M., Yang, E.X., Am Ende, C.W., Arnold, E.P., Head, J.L., Jenkinsonb, S., Lebel, L.A., Liras, S., Pandit, J., Samas, B., Vajdos, F., Simons, S.P., Evdokimova, A., Mansour, M., Menniti, F.S.	_

3.1.2 Alignment

The protein sequence of 1SO2,1TAZ and 4NPV crystal structures were extracted and downloaded into Molsoft ICM-PRO to be used as templates for the homology models. Using the ICM alignment tool, the PDE3A sequence was aligned with the template sequences of 1SO2, 1TAZ and 4NPV. The sequence of the PDE3A enzyme consists of 1141 amino acid residues, while the templates had 363, 322 and 323 residues (catalytic domain) respectively. Consequently, the alignment of the query sequence to its template was mainly focused on the catalytic domain of the enzyme. The sequence for the N-terminal of the PDE3A enzyme was cropped out of the alignments. The remaining sequence consisted of the amino acid residues roaming from A660-Q114. Thus, the sequence length was reduced from 1141 to 482 amino acids in this study. The gaps in the alignment were compressed using the ICM inbuilt tool. The alignments were not further adjusted.

```
75% pP=55.4                    ................#-####-.#DS##E.#..WNFPIF-LVE.#G.K.GRILSQV.Y.LF
PDE3A_HUMAN_1    1    APETMMFLDKPILAPEPLVMDNLDSIMEQLNTWNFPIFDLVENIGRKCGRILSQVSYRLF
v1so2_a        659    --------------LDLILVEEYDSLIEKMSNWNFPIFELVEKMGEKSGRILSQVMYTLF
v1so2_a

                               .D.GL#E#FKIP...FMNYF.ALE.GYRDIPYHNRIHATDVLHAVWYLTT.P#PGL..##
PDE3A_HUMAN_1   61    EDMGLFEAFKIPIREFMNYFHALEIGYRDIPYHNRIHATDVLHAVWYLTTQPIPGLSTVI
v1so2_a        705    QDTGLLEIFKIPTQQFMNYFRALENGYRDIPYHNRIHATDVLHAVWYLTTRPVPGLQQIH
v1so2_a

                               N.................G.#.Y#.SK.#...D-.YGCLS.NIPALELMALYVAAAMHDYD
PDE3A_HUMAN_1  121    NDHGSTSDSDSDSGFTHGHMGYVFSKTYNVTDDKYGCLSGNIPALELMALYVAAAMHDYD
v1so2_a        765    NG--------------GRIAYISSKSCSNPDESYGCLSSNIPALELMALYVAAAMHDYD
v1so2_a

                               HPGRTNAFLVAT.APQAVLYNDRSVLENHHAA.AWNL##SRPEYNFL#.LDHVEFK.FRF
PDE3A_HUMAN_1  181    HPGRTNAFLVATSAPQAVLYNDRSVLENHHAAAAWNLFMSRPEYNFLINLDHVEFKHFRF
v1so2_a        825    HPGRTNAFLVATNAPQAVLYNDRSVLENHHAASAWNLYLSRPEYNFLLHLDHVEFKRFRF
v1so2_a

                               LVIEAILATDLKKHFDF#A.FN.K#ND....GI-W.NENDRLLVCQ#CIKLADINGPAK#
PDE3A_HUMAN_1  241    LVIEAILATDLKKHFDFVAKFNGKVND--DVGIDWTNENDRLLVCQMCIKLADINGPAKC
v1so2_a        885    LVIEAILATDLKKHFDFLAEFNAKANDVNSNGIEWSNENDRLLVCQVCIKLADINGPAKV
v1so2_a

                               +-LHL.WT-GIVNEFYEQGDEEA.LGLPISPFMDRS.PQLA.LQESFI.HIVGPLCNSYD
PDE3A_HUMAN_1  299    KELHLQWTDGIVNEFYEQGDEEASLGLPISPFMDRSAPQLANLQESFISHIVGPLCNSYD
v1so2_a        945    RDLHLKWTEGIVNEFYEQGDEEANLGLPISPFMDRSSPQLAKLQESFITHIVGPLCNSYD
v1so2_a

                               .AGL#PG.W#E.........................................RR+I#CQ#..
PDE3A_HUMAN_1  359    SAGLMPGKWVEDSDESGDTDDPEEEEEEAPAPNEEETCENNESPKKKTFKRRKIYCQITQ
v1so2_a       1005    AAGLLPGQWLE-----------------------------------------SRRRIFCQLMH
v1so2_a

                               HL..NHK#WK...................................................
PDE3A_HUMAN_1  419    HLLQNHKMWKKVIEEEQRLAGIENQSLDQTPQSHSSEQIQAIKEEEEEKGKPRGEEIPTQ
v1so2_a       1064    HLTENHKIWK---------------------------------------------------
v1so2_a

                               ....
PDE3A_HUMAN_1  479    KPDQ
v1so2_a               ----
v1so2_a
```

Figure 6. *Sequence alignment of PDE3A with 1SO2 used for the homology modeling. Dark green and green areas are fully conserved and have identical sequence residues with template. Yellow areas are semi conserved, and white areas are the non-conserved regions. The red bars symbolize the alfa helical secondary structure while the purple bars show non conical helices.*

19

```
37% pP=16.7          #.P.#...#..##..L..W.F.#F.L...#...#...L..#.#.L#..#.L#..FKIP.
PDE3A_HUMAN_1    15  PEPLVMDNLDSIMEQLNTWNFPIFDLVENIGRKCGRILSQVSYRLFEDMGLFEAFKIPI
v1taz_a         146  VGPTYSTAVLNCLKNLDLWCFDVFSLNQAADDHA---LRTIVFELLTRHNLISRFKIPT
v1taz_a               ⚬━━━━  ━━━━━━ ⚬━━━━━━━━━ ⚬━ ━━━━━━━━━━━━⚬

                     ..#M.##.ALE.GY..#..PYHN.IHA.DV...V#.#... .G#.H CLS.....#EL#A
PDE3A_HUMAN_1    74  REFMNYFHALEIGYRDI--PYHNRIHATDVLHAVWYLTTQ SGFTH CLSGNIPALELMA
v1taz_a         202  VFLMSFLDALETGYGKYKNPYHNQIHAADVTQTVHXFLLR TGMVH CLS----EIELLA
v1taz_a              ⚬━━━━━━━━━━━━  ⚬━━━━━━━━━ ━━━━━━━━━⚬⚬━⚬⚬  ⚬━━━━━

                     ###AAA#HDY-H.G.TN.F##.T....A##YNDRSVLENHH#..##.L.M...E#N##IN
PDE3A_HUMAN_1   170  LYVAAAMHDYDHPGRTNAFLVATSAPQAVLYNDRSVLENHHAAAAWNLFMSRPEYNFLIN
v1taz_a         256  IIFAAAIHDYEHTGTTNSFHIQTKSECAIVYNDRSVLENHHISSVFRL-MQDDEMNIFIN
v1taz_a              ⚬━━━━━━━━ ⚬━━━━ ⚬━━━━ ⚬━━━━━━━━━ ⚬━ ⚬━━━━━━

                     L...EF..#R#LVIE##LATD#..HF..V..#...#.. ..D+#.##.###.#ADI..P.
PDE3A_HUMAN_1   230  LDHVEFKHFRFLVIEAILATDLKKHFDFVAKFNGKVND ENDRLLVCQMCIKLADINGPA
v1taz_a         315  LTKDEFVELRALVIEMVLATDMSCHFQQVKTMKTALQQ RIDKPKALSLLLHAADISHPT
v1taz_a              ⚬━ ━━━━━━━━━━━━━━ ⚬━━━━━ ━━━━━━━━━━━⚬   ⚬━━━━━━━━ ━━⚬

                     K...#H..WT..##.EF#.QGD.EA.LGLP R....#A..Q..FI.#IV.P.#..# TD.
PDE3A_HUMAN_1   297  KCKELHLQWTDGIVNEFYEQGDEEASLGLP RSAPQLANLQESFISHIVGPLCNSY TDD
v1taz_a         376  KQWLVHSRWTKALMEEFFRQGDKEAELGLP RTSTLVAQSQIGFIDFIVEPTFSVL TDV
v1taz_a              ⚬━━━━━━━━━━━━━━━━━━━━━━⚬ ⚬━━━━━━━━━━━━━━━━━━━━⚬ ⚬━━

                     #E.... ...P....F+...#.......#..N...WK..#..
PDE3A_HUMAN_1   380  PEEEEE NESPKKKTFKRRKIYCQITQHLLQNHKMWKKVIEE
v1taz_a         440  AEKSVQ DPNPDVVSFRSTWV-----KRIQENKQKWKERAAS
v1taz_a              ⚬━━━━ ⚬━━━━ ⚬━━━━━━━━ ⚬━━━━━━━━━━⚬
```
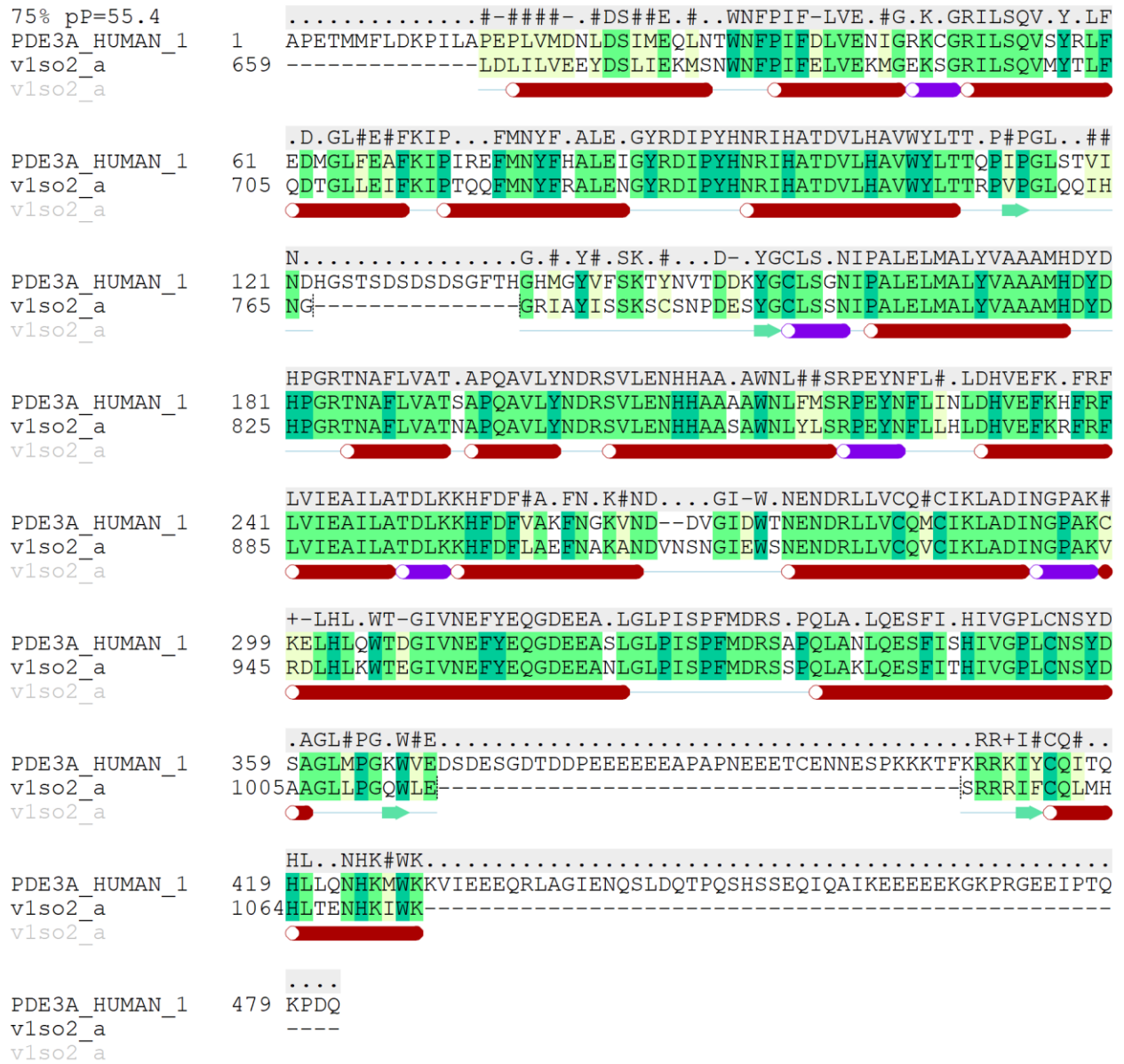
Figure 7. *Sequence alignment of PDE3A with 1TAZ used for the homology modeling. Dark green and green areas are fully conserved and have identical sequence residues with template. Yellow areas are semi conserved, and white areas are the non-conserved regions. The red bars symbolize the alfa helical secondary structure while the purple bars show non conical helices.*
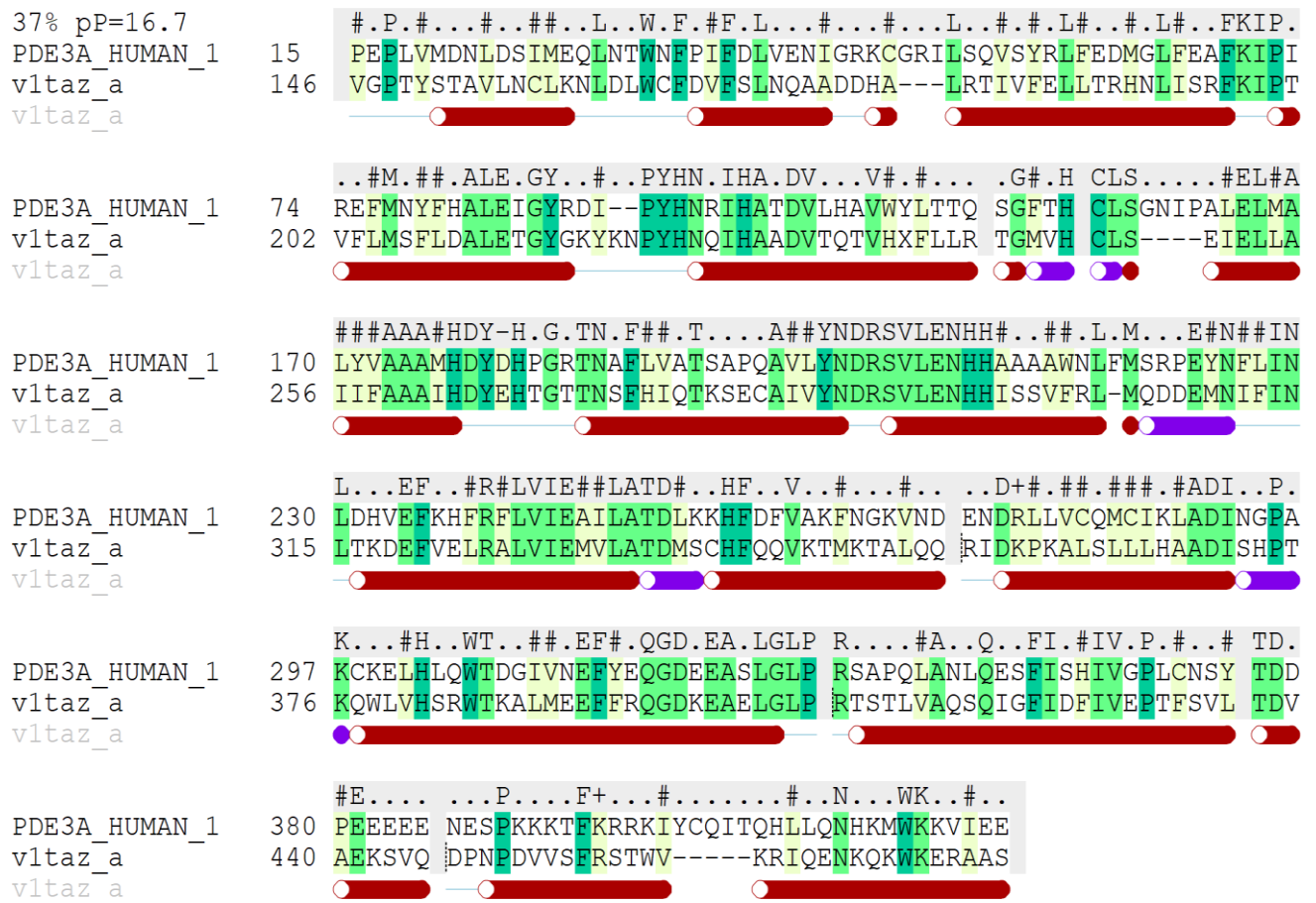
20

```
37% pP=18.0                .........................#..##..L..W.F.#F.L...#...#...L..#.#.L#
PDE3A_HUMAN_1      1   APETMMFLDKPILAPEPLVMDNLDSIMEQLNTWNFPIFDLVENIGRKCGRILSQVSYRLF
v4npv_a            1   ------------------STAVLNCLKNLDLWCFDVFSLNQAADDHA---LRTIVFELL
v4npv_a

                      ..#.L#..FKIP...#M.##.ALE.GY..#..PYHN.IHA.DV...V###..........
PDE3A_HUMAN_1     61   EDMGLFEAFKIPIREFMNYFHALEIGYRDI--PYHNRIHATDVLHAVWYLTTQPIPGLST
v4npv_a           39   TRHNLISRFKIPTVFLMSFLDALETGYGKYKNPYHNQIHAADVTQTVHCFLLR-------
v4npv_a

                      ................G#.H....................CLS.....#EL#A###AAA#HD
PDE3A_HUMAN_1    119   VINDHGSTSDSDSDSGFTHGHMGYVFSKTYNVTDDKYGCLSGNIPALELMALYVAAAMHD
v4npv_a           92   --------------TGMVH------------------CLS----EIELLAIIFAAAIHD
v4npv_a

                      Y-H.G.TN.F##.T....A##YNDRSVLENHH#..##.L.M...E#N##INL...EF..#
PDE3A_HUMAN_1    179   YDHPGRTNAFLVATSAPQAVLYNDRSVLENHHAAAAWNLFMSRPEYNFLINLDHVEFKHF
v4npv_a          115   YEHTGTTNSFHIQTKSECAIVYNDRSVLENHHISSVFRL-MQDDEMNIFINLTKDEFVEL
v4npv_a

                      R#LVIE##LATD#..HF..V..#...#.....#-.......L....###.#ADI..P.K.
PDE3A_HUMAN_1    239   RFLVIEAILATDLKKHFDFVAKFNGKVNDDVGIDWTNENDRLLVCQMCIKLADINGPAKC
v4npv_a          174   RALVIEMVLATDMSCHFQQVKTMKTALQQ---LERIDKPKAL---SLLLHAADISHPTKQ
v4npv_a

                      ..#H..WT..##.EF#.QGD.EA.LGLP#SP##DR....#A..Q..FI.#IV.P.#..#.
PDE3A_HUMAN_1    299   KELHLQWTDGIVNEFYEQGDEEASLGLPISPFMDRSAPQLANLQESFISHIVGPLCNSYD
v4npv_a          228   WLVHSRWTKALMEEFFRQGDKEAELGLPFSPLCDRTSTLVAQSQIGFIDFIVEPTFSVLT
v4npv_a

                      .#........................E..#.P...............P....F+...#......
PDE3A_HUMAN_1    359   SAGLMPGKWVEDSDESGDTDDPEEEEEEAPAPNEEETCENNESPKKKTFKRRKIYCQITQ
v4npv_a          288   DVA---------------------EKSVQP-----------PDVVSFRSTWV-----K
v4npv_a

                      .#..N...WK..#.............................................
PDE3A_HUMAN_1    419   HLLQNHKMWKKVIEEEQRLAGIENQSLDQTPQSHSSEQIQAIKEEEEEKGKPRGEEIPTQ
v4npv_a          309   RIQENKQKWKERAAS-------------------------------------------
v4npv_a

                      ....
PDE3A_HUMAN_1    479   KPDQ
v4npv_a               ----
v4npv_a
```
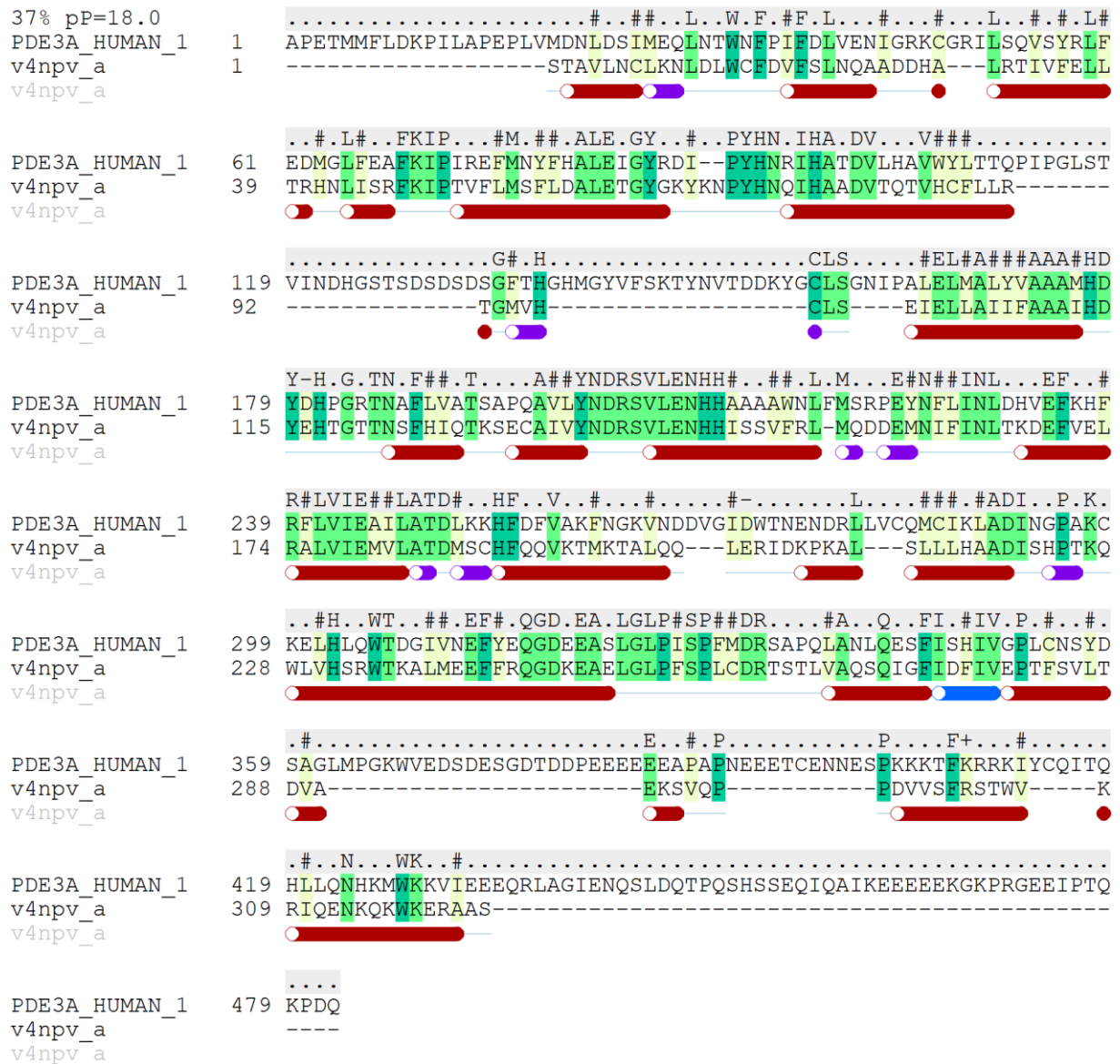
Figure 8. Sequence alignment of PDE3A with 4NPV used for the homology modeling. Dark green and green areas are fully conserved and have identical sequence residues with template. Yellow areas are semi conserved, and white areas are the non-conserved regions. The red bars symbolize the alfa helical secondary structure while the purple bars show non conical helices.

3.1.3 Building PDE3 models

Three homology models of the catalytic domain of the human PDE3A were built based on three different crystal structures (1SO2, 1TAZ and 4NPV). Two of the three crystal structures (1TAZ and 4NPV) that were chosen are made up of the sequence of the same enzyme, but these were crystalized in differing complexes. The crystal structure 1TAZ is a structure of the catalytic domain of the human PDE1B. This structure is not bound to an inhibitor unlike the others. 1TAZ crystal structure consists of 365 residues and has a resolution of 1,77 Å. The structure 4NPV is a crystal structure of human PDE1B bound to inhibitor 7A (6,7,8-trimethoxy-N-(pentan-3-yl) quinazolin-4-amine). The crystal is synthetized at a resolution of 2,40 Å and consists of 369 residues. Finally, the 1SO2 crystal structure is a structure of the catalytic domain in the human PDE3B in a complex with dihydropyridine inhibitor. The structure of PDE3B made at 2,40 Å resolution by using x-ray diffraction and has a sequence length of 420 residues. Unlike the other chosen templates with a single chain, the 1SO2 structure consists of 4 chains (chain A-D). The single chain A was chosen as a template in building the homology model. The molecules were built with surrounding molecules and active site ligands from the template included. The resulting models were homology models of the catalytic domain of the PDE3A enzyme (residue 660-1141) and not the complete enzyme entity.

3.1.4 Refinement of models

The models of the PDE3A enzyme were refined simultaneously as the models were built. The full model builder feature in ICM refines both sidechains and loops when building and constructing the homology models.

3.1.5 Evaluation of models

The evaluation of the models was carried out using SAVES meter server software (https://servicesn.mbi.ucla.edu/SAVES/). In this paper, model reliability was examined using both PROCHECK and ERRAT. PROCHECK results are presented in a Ramachandran plot. The purpose of this plot is to visualize and thus evaluate the reliability of the structural stereochemistry of the models. ERRAT, on the other hand, is used to check the stereochemical interactions of the models. Finally, the structures and templates were eventually compared to each other, and a root mean square deviation (RMSD) value was calculated using ICM-PRO.

3.2   Uncovering active site residues

One of the main aims of this research was to pinpoint some of the active site residues that contribute to ligand binding. The most reliable model as presumed through the evaluation tests was further assessed for active site information. The PDE3A model was used as an aid to identify conserved residues in the catalytic domain that may be essential for ligand binding.

4 Results and discussion

4.1 Homology modeling

Prior to this study, there was no existing 3D structures of the PDE3A enzyme that had been published. Recent studies have highlighted the clinical relevance of drugs that can modify the activity of PDE3A (3, 5). Therefore, the homology modeling approach was chosen for the sake creating a model to assist future drug development. Structural representations of the PDE3A enzyme is scarce and thus models act as major asset for further modeling progression and evolution of PDE3A drug inhibitors that are suitable for hypothermic patients. A 3D structure of the PDE3A enzyme will also provide information of the ligand binding interactions which is important for developing drugs with high binding affinity. The homology models of the PDE3A enzyme are therefore constructed for provisional purposes.

4.1.1 Template search

The crystal structures of the templates that were used to build the homology models of PDE3A have the PDB IDs 1SO2, 1TAZ and 4NPV. The crystal structure of a protein is a better representation of the real structure and is therefore more suitable as a template compared to a scientifically produced model. Thus, the search for templates were limited to only find crystalized structures in the PDB before making the models. The PDE3A models were made by using the most structurally similar crystal structures that have been published in the PDB. According to the phylogenic tree of the PDE enzyme families, the PDE3B is the closest relative to PDE3A, followed by the PDE1B (see Figure 1) Therefore, the templates that were chosen for the homology models, produce the most accurate results.

4.1.2 Sequence identity, similarity and alignments

The sequence identity of the chosen crystal structures, 1SO2, 1TAZ and 4NPV, were 69%, 34% and 34% and had a resolution of 2,40Å, 1,77Å and 2,40Å respectively (Table 2). The composition of the amino acid sequence and the order of the amino acid residues in a polypeptide is pivotal to the mold of the resulting secondary structure of a protein (28). Concurrently, models that are constructed based on templates with high sequence similarity, is accountable to model accuracy (34). The 1SO2-based model has a good sequence identity with its corresponding template and is therefore most reliable. However, 1TAZ and 4NPV-based models had a slightly lower sequence identity compared to their corresponding models ($< 50\%$).

24

The sequence similarity of the models 1SO2, 1TAZ and 4NPV were 84%, 47% and 47% respectively (table 2) indicating good resemblance to the templates. The sequence templates 1TAZ and 4NPV share the same sequence identity (34%) and similarity (47%) (compared to PDE3A sequence), the reason being the fact that they are crystals of identical enzymes. The difference between them is that 1TAZ is crystalized while unbound to an inhibitor, while 4NPV is crystalized with inhibitor 7A (6,7,8-trimethoxy-N-(pentan-3-yl) quinazolin-4-amine.

Due to limited query coverage of the templates to the entire entity of the PDE3A sequence, the models conducted represent only the catalytic domain of the PDE3A enzyme. Nevertheless, the catalytic domain is known to exhibit the active properties of the enzyme, making it the only part of the enzyme of topic relevance. Also, previous studies have shown that when cropping the PDE3A enzyme sequence at residue 660, the partial enzyme (catalytic site) remains active (35).The protein sequence of the PDE3A human enzyme was trimmed at residue A660 to achieve this. The sequence alignments were automated using ICM and required minimum alterations.

4.1.3   3D structure of PDE3A
The final models of the PDE3A enzyme are named "1SO2-based model", "1TAZ-based model" and "4NPV-based model" as shown in Figure 9 (left). These models visualize the secondary structure elements of the enzyme. The structure consists mainly of alfa helices connected by loops. These secondary structures are visibly highly similar to the 3D crystal structure of the templates. This can be seen for all the three models (see Figure 11). The parts without secondary structures is mainly due to absent template coverage (gaps). The resulting model lacks the N-terminal phosphorylation site of the PDE3A enzyme, and the TM hydrophobic loops as mentioned earlier. The constructed homology models contain structural information of the highly conserved C-terminal with the distinctive 44 amino acid insert and the active binding site of the PDE3A enzyme.

4.2   Model Evaluations

4.2.1   PROCHECK

According to PROCHECK statistics one can assume to have a model of high quality when over 90% of the residues reside in their most favorable state represented by the Ramachandran plot (36). Table 3 summarizes the Ramachandran plot statistics. 1TAZ-based model has 90,7% residues in the most favored regions, 8,2% residues in additionally allowed regions, 1,2% residues in generously allowed regions and 0,0% residues in disallowed regions. 1SO2-based model has 89,5% residues in the most favored regions, 10,0% residues in additionally allowed regions, 0,5% residues in generously allowed regions and 0,0% residues in the disallowed regions, and finally 4NPV-based model has 86,9% residues in the most favored regions, 11,0% residues in additionally allowed regions, 1,6% residues in generously allowed regions and 0,5% residues in disallowed regions. The results show that 1SO2 and 4NPV-based models are close to the 90% limit (89,5% and 86,9% respectively) and are therefore presumably of satisfactory quality, while 1TAZ model is of high quality (90,7% in favorable regions). Though 1SO2-based model had the highest sequence similarity to its template, 1TAZ-based model is the most stable according to this diagram. This highlights the fact that high sequence similarity is not the solely relevant factor associated with model accuracy.

The aim of this study is to compile the information relevant to inhibitor binding. Therefore, it was most preferable that the templates are bound to inhibitors for high quality models. The templates bound to inhibitors are 1SO2 and 4NPV while the template structure 1TAZ is unbound. It is unknown whether the residue stability of 1TAZ-based model is due to using an unbound enzyme as a model template. In conclusion, according to the results of the Ramachandran plot, the 1TAZ-based model is the most suitable for use in future studies.

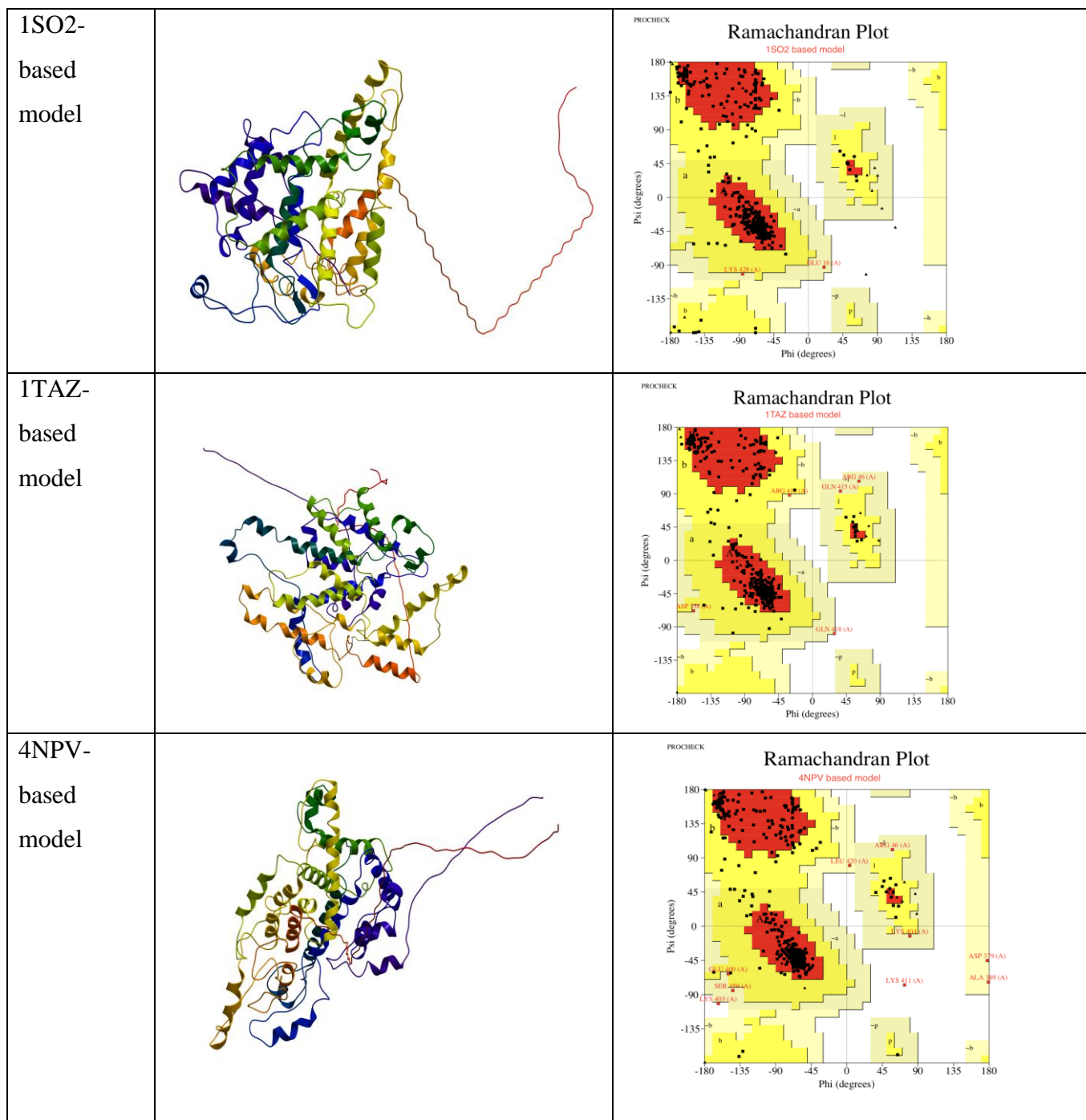|		
1SO2-based model		
1TAZ-based model		
4NPV-based model		

Figure 9. Left: The secondary structure of the constructed models of PDE3A shown as ribbons. This figure was generated using ICM. The structure is colored starting from the amino acid residue 660 (red) to residue 1141 (blue). The first model is 1SO2-based, the second model is 1TAZ-based, and the third model is 4NPV-based. Right: The Ramachandran plots of all three models generated via PROCHECK. The Ramachandran plot visualizes the areas in which the residues are most favored. The red areas are the most favored, yellow is the additionally allowed areas, the generously allowed areas is pale yellow and finally the disallowed areas are white.

Table 3. *PROCHECK Ramachandran plot summary for 1SO2, 1TAZ and 4NPV-based models.*

	Most favoured regions	Additionally allowed regions	Generously allowed regions	Disallowed regions
1SO2-based model	89,5	10,0	0,5	0,0
1TAZ-based model	90,7	8,2	1,2	0,0
4NPV-based model	86,9	11,0	1,6	0,5

4.2.2 ERRAT

The ERRAT test is a validating procedure that assesses the non-bonded interactions between different atom or molecule types. Errors in a model can lead to inadequate atom distribution. ERRAT calculates and distinguishes these errors from the correct determined regions and produces a summarizing score that is reflective of the overall quality factor. Thus high ERRAT scores corresponds with higher quality (29). In general, an overall quality factor over 50% is acceptable (37). The 1SO2,1TAZ and 4NPV-based models have an ERRAT score of 87,4 %, 85,4% and 79,9% respectively (Figure 10). All the models are therefore within the acceptable limits and are therefore of good stereochemical quality. According to the ERRAT scores, 1SO2-based model has the highest overall quality factor, followed by the 1TAZ-based model, and finally the 4NPV-based model provided the lowest overall quality factor. In conclusion the 1SO2- based model of the PDE3A enzyme has the least errors and is thus the model with highest stereochemical quality.
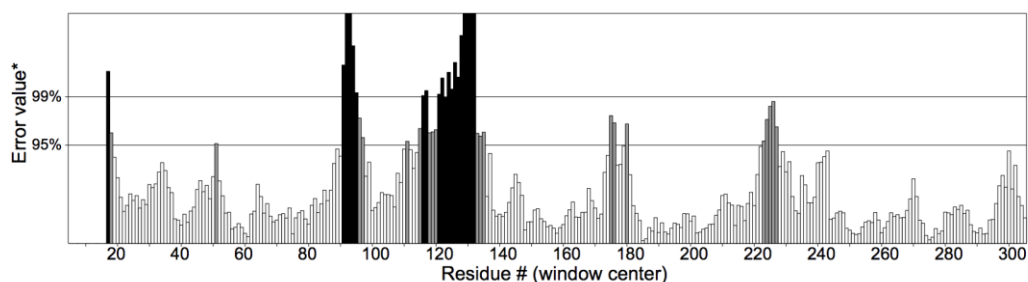
1SO2-based model

Overall quality factor**: 87.441
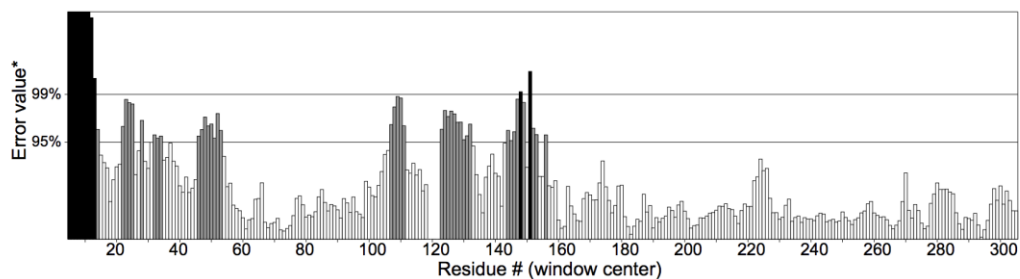
1TAZbased model

Overall quality factor**: 85.442

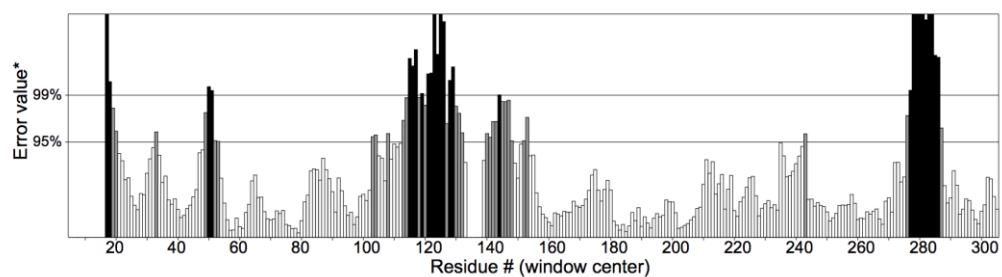**4NPV-based model**

Overall quality factor**: 79.952

Figure 10. *ERRAT plots for the1SO2, 1TAZ and 4NPV-based models. The two horizontal lines drawn on the error axis show the confidence interval of which it is possible to reject regions that exceed error value. An overall quality value above 95% is expected for high quality models with high resolution (<2.5Å) (ERRAT).*

4.2.3 RMSD

The three models were superimposed on their templates to visualize the main structural differences (see Figure 11). Primarily the main differences can be seen in the unaligned and un-conserved areas of the catalytic domain. The RMSD value is calculated based on the differences of C-alpha atoms between the structure and template. 1SO2-based model with the highest sequence identity of 69% has the lowest RMSD value (0,116Å), followed by 1TAZ-based model with 37% sequence identity (0,124Å) and the 4NPV-based model with a sequence identity of 37% (0,137Å) (Table 4). A low calculated RMSD value signifies few structural differences and is a sign of a good model. Therefore, the results of RMSD compared to sequence identity are as expected; the homology models with high sequence identity have the lowest RMSD values. Low RMSD between the models and their corresponding templates indicate minor structural differences.

The RMSD of the three superimposed models, calculated by ICM-PRO is 0,853 (Table 4). The figure of the superimposed homology models (Figure 11) show that there are few structural differences between the three models. The RMSD between the models is considerably low. These results are credible because the model templates are neighboring family members as represented in Figure 1. As expected, the aberrant parts correspond to the parts that did not have sequence coverage (gaps) in the alignments. Overall, the models fit well into the main template structures regardless.
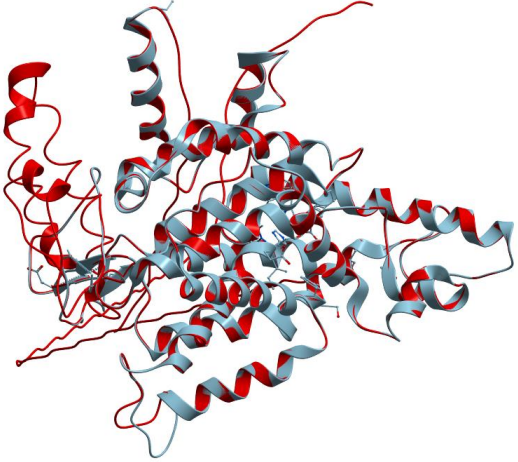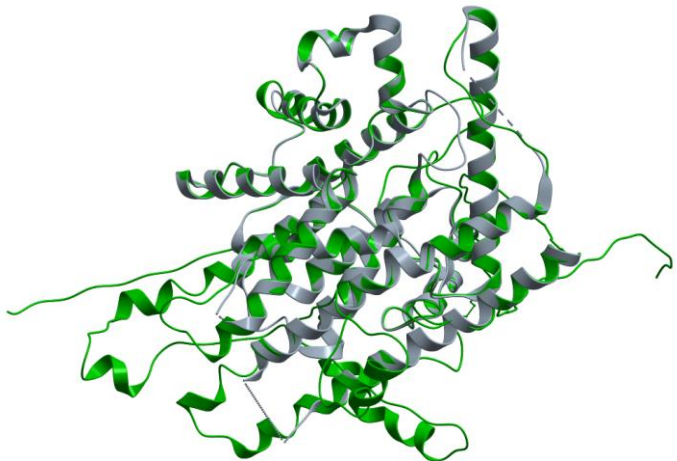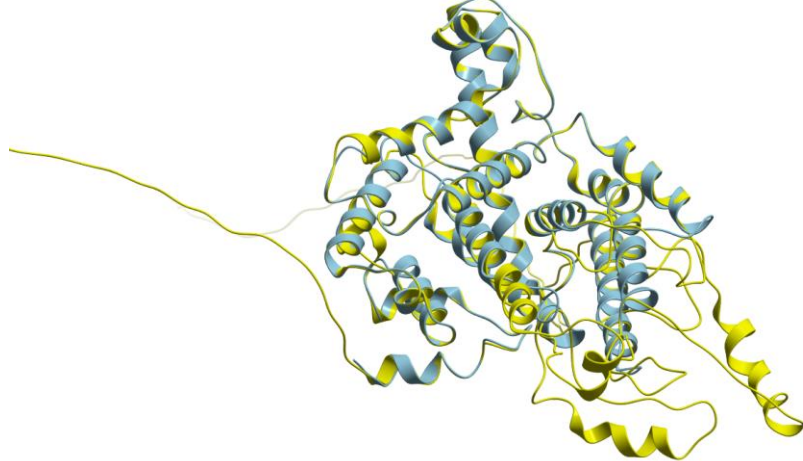
1SO2-based model superimposed on 1SO2 crystal structure	
1TAZ-based model superimposed on 1TAZ crystal structure	
4NPV-based model superimposed on 4NPV crystal structure	

Figure 11. Superimposition of the models and their corresponding templates. Top: 1SO2-based model (red), middle: 1TAZ-based model (green) and 4NPV-based models (yellow). The templates are colored grey.
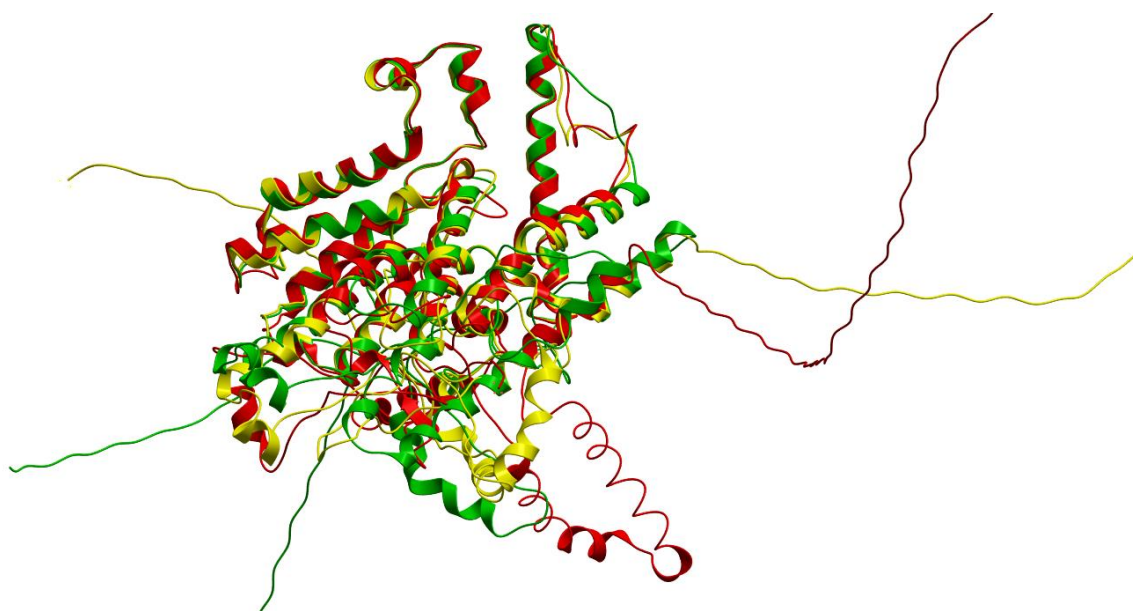
31

Figure 12. *The superimposition of the three homology models constructed. 1SO2 is colored in red, 1TAZ is colored in green and 4NPV is colored in yellow for representation.*

Table 4. *Calculated RMSD for the homology models*

	1SO2-based model	1TAZ-based model	4NPV-based model	All three models superimposed
RMSD (Å)	0,116	0,124	0,137	0,853

4.3 Assessing model quality

The 1SO2 template has the highest sequence identity (69%) to the PDE3A sequence as seen in table 2, but surprisingly the unbound 1TAZ-based model has most stable residue conformations (90,7%) as viewed in the Ramachandran plot (Figure 9). However, the ERRAT results and the RMSD values advocate for the 1SO2 model quality. Though the 4NPV-based model is of satisfactory quality, the model evaluations reveal that 1SO2- and 1TAZ-based models are more reliable. The high Ramachandran values of the 1TAZ-based model could presumable be a result of the missing ligand within the model. The absence of a bound ligand acquires more space for the residues. The residues are therefore presumably not constricted and might result in more stable conformations. Moreover, since the main interest of this thesis is to access ligand binding interactions within the active site of the PDE3A enzyme to, it is applicable to use a ligand bound based model such as the 1SO2-based model. According to model evaluations, 1SO2 is

consequently be the best model of choice for future studies due to high sequence similarity, stereochemical quality, low RMSD and stable residue conformations.

4.4 Ligand binding residues of PDE3A

As a result of the model evaluations, the 1SO2-based homology model was used to visualize the residues in the active site of the PDE3A enzyme within the vicinity of the dihydropyridine inhibitor. Using this model, a list of active site residues that potentially are associated with ligand binding was conducted (Table 5).
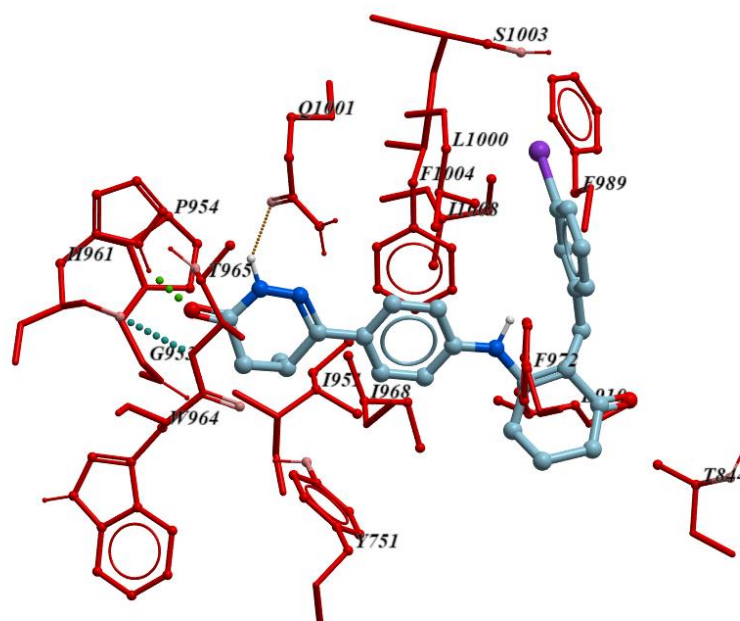

Figure 13*. Active site interactions of the 1SO2-based model. The active site residues are colored red and numbered. The ligand (dipyridamole) is colored grey. Hydrogen bond interactions are displayed as dotted lines.*

Table 5*. List of conserved active site residues found in PDE3A model (1SO2-based model).*

	Residues found in active site of 1SO2-based model
Conserved residues	T844, L919, D950, I951, N952, G953, L960, Q963, T965, I968 M990, L1000, Q1001, E1002, S1003, I1008, V1009
Super conserved residues	Y751, H752, P954, H961, W964, F972, F989, F1004, H1007

33

Table 5 is an overview of the active site residues that are found to be involved in ligand pocket interactions. All of the residues that are shown to be in the active site are either conserved or super conserved. These residues in the model homology model were also perfectly aligned to the template (1SO2). Figure 13 is a visual representation of the active site residues and their positions relative to dipyridamole. The ligand-enzyme interactions of the PDE3A model are presumably highly similar to PDE3B ligand binding (template) due conserved residue positions. Mutagenesis studies of the PDE3 interaction sites, revealed that the mutation of residues Y751, T844, D950, F972, Q975 and F1004 affect both Km and Ki compared to the wild type(21, 26). These studies highlight the importance of these residues to ligand binding and enzymatic activity. According to Figure 13, there are hydrogen bond reactions between the enzyme and ligand (dipyridamole). This indicates that an aqueous environment will affect the binding affinity of the enzyme. In conclusion, a suggestion for future studies is to further investigate the interactions between the featured active site residues and a potential inhibitor to increase binding specificity and affinity.

5 Conclusion

Three homology models have been made in order to study the ligand binding properties of the PDE3A enzyme due to the lack of its crystalized 3D structure. The models created are of high quality and with good sequence similarity to its templates. The 1SO2-based model was found to be the most reliable according to the model evaluations. By means of this model, the presumably important amino acids for ligand binding have been elucidated. The highly conserved residues Y751, T844, D950, F972, Q975 and F1004 are found within the vicinity of the ligand in both the 1SO2-based model and its template. These findings may be of value to facilitate PDE3A inhibitor drugs that are effective and specific for use in hypothermic conditions.

6 Future studies

Thanks to this research, the first step to the development of PDE3A inhibitors is established. A homology model of high quality can be used as a guide to generate compounds from e-molecules that act as candidates for virtual ligand screening. The 1SO2-based model of the PDE3A enzyme can be used as a template for identification of hit compounds. The compounds that exhibit high affinity for the active site residues that are essential to enzyme ligand binding can be further tested as potential candidates of PDE3A enzyme inhibition. During hypothermia pharmacokinetic processes in the body are often delayed. Thus when the body is rewarmed and the pharmacokinetic conditions are normalized, there is often a need for dose adjustments of drugs (8, 9, 36). In order for the future PDE3A inhibitors to be specialized for use under hypothermic conditions, a short $T_{1/2}$ is preferable so that the drug dose can be adjusted after rapid changes in patient condition. Therefore, the potential PDE3A inhibitors drug candidates must be checked for putative ADMET properties, subjected molecular dynamics simulations at temperatures below 30 °C, and tested in vitro for short half-life.

7   References

1.   Lee DI, Kass D. Phosphodiesterases and Cyclic GMP Regulation in Heart Muscle. Physiology. 2012;27(4):248-58.
2.   Omori K, Kotera J. Overview of PDEs and Their Regulation. Circulation Research. 2007;100(3):309-27.
3.   Dietrichs ES, Kondratiev T, Tveita T. Milrinone ameliorates cardiac mechanical dysfunction after hypothermia in an intact rat model. Cryobiology. 2014;69(3):361-6.
4.   Tveita T, Sieck GC. Effects of milrinone on left ventricular cardiac function during cooling in an intact animal model. Cryobiology. 2012;65(1):27-32.
5.   Dietrichs ES, Håheim B, Kondratiev T, Sieck GC, Tveita T. Cardiovascular effects of levosimendan during rewarming from hypothermia in rat. Cryobiology. 2014;69(3):402-10.
6.   Saad H, Aladawy M. Temperature management in cardiac surgery. Glob Cardiol Sci Pract. 2013;2013(1):44-62.
7.   Dietrichs ES. Hvorfor stopper hjertet når det blir for kaldt? Aftenposten. 2015, April 22.
8.   Håheim B, Kondratiev T, Dietrichs ES, Tveita T. The beneficial hemodynamic effects of afterload reduction by sodium nitroprusside during rewarming from experimental hypothermia. Cryobiology. 2017;77:75-81.
9.   Dietrichs ES, Sager G, Tveita T, Dietrichs ES. Altered pharmacological effects of adrenergic agonists during hypothermia. Scandinavian journal of trauma, resuscitation and emergency medicine. 2016;24(1):143-.
10.   Wyckoff MH, Aziz K, Escobedo MB, Kapadia VS, Kattwinkel J, Perlman JM, et al. Part 13: Neonatal Resuscitation: 2015 American Heart Association Guidelines Update for Cardiopulmonary Resuscitation and Emergency Cardiovascular Care (Reprint). Pediatrics. 2015;136 suppl 2(s2):S196-S218.
11.   Pinsky MR, Teboul J-L, Vincent J-L. Hemodynamic Monitoring. Cham: Springer International Publishing : Imprint: Springer; 2019.
12.   Menezes-Rodrigues FS, Pires-Oliveira M, Duarte T, Paredes-Gamero EJ, Chiavegatti T, Godinho RO. Calcium influx through L-type channels attenuates skeletal muscle contraction via inhibition of adenylyl cyclases. European Journal of Pharmacology. 2013;720(1-3):326-34.
13.   Foye WO, Lemke TL, Williams D. Foye's principles of medicinal chemistry. 6th ed. edited by Thomas L. Lemke, David Williams ; assistant editors, Victoria F. Roche, S. William Zito. ed. Philadelphia: Wolters Kluwer/Lippincott Williams & Wilkins; 2008.
14.   Johnson WB, Katugampola S, Able S, Napier C, Harding SE. Profiling of cAMP and cGMP phosphodiesterases in isolated ventricular cardiomyocytes from human hearts: Comparison with rat and guinea pig. Profiling of cAMP and cGMP phosphodiesterases in isolated ventricular cardiomyocytes from human hearts: Comparison with rat and guinea pig. 2012;90(9):328-36.
15.   Karabencheva-Christova T. Biomolecular Modelling and Simulations: San Diego: Elsevier Science & Technology; 2014.
16.   Henderson G, Flower RJ, Ritter JM, Dale MM, Rang HP. Rang and Dale's pharmacology. 8th ed. ed. Edinburgh: Elsevier Churchill Livingstone; 2016.
17.   Boswell-Smith V, Spina D, Page CP. Phosphodiesterase inhibitors. British journal of pharmacology. 2006;147 Suppl 1:S252.
18.   Fossa P, Giordanetto F, Menozzi G, Mosti L. Structural basis for selective PDE 3 inhibition: a docking study. Quantitative Structure-Activity Relationships. 2002;21(3):267-75.

19.   Matthew M, Faiyaz A, Emilio H. Functions of PDE3 Isoforms in Cardiac Muscle. Journal of Cardiovascular Development and Disease. 2018;5(1):10.

20.   Meacci E, Taira M, M Moos, Jr., Smith CJ, Movsesian MA, Degerman E, et al. Molecular cloning and expression of human myocardial cGMP-inhibited cAMP phosphodiesterase. Proceedings of the National Academy of Sciences of the United States of America. 1992;89(9):3721.

21.   Zhang W, Ke H, Tretiakova AP, Jameson B, Colman RW. Identification of overlapping but distinct cAMP and cGMP interaction sites with cyclic nucleotide phosphodiesterase 3A by site-directed mutagenesis and molecular modeling based on crystalline PDE4B. Protein Science. 2001;10(8):1481-9.

22.   Maass PG, Aydin A, Luft FC, Schächterle C, Weise A, Stricker S, et al. PDE3A mutations cause autosomal dominant hypertension with brachydactyly. Nature genetics. 2015;47(6):647-53.

23.   Martin E, Hine R. UniProt. 7 ed: Oxford University Press; 2015.

24.   Wechsler J, Choi Y-H, Krall J, Ahmad F, Manganiello VC, Movsesian MA, et al. Isoforms of cyclic nucleotide phosphodiesterase PDE3A in cardiac myocytes. The Journal of biological chemistry. 2002;277(41):38072-8.

25.   Scapin G, Patel SB, Chung C, Varnerin JP, Edmondson SD, Mastracchio A, et al. Crystal Structure of Human Phosphodiesterase 3B: Atomic Basis for Substrate and Inhibitor Specificity †. Biochemistry. 2004;43(20):6091-100.

26.   Zhang W, Ke H, Colman RW, Zhang W. Identification of interaction sites of cyclic nucleotide phosphodiesterase type 3A with milrinone and cilostazol using molecular modeling and site-directed mutagenesis. Molecular pharmacology. 2002;62(3):514-20.

27.   Richard E. Klabunde PD. Phosphodiesterase inhibitors: General pharmacology of camp-dependent phosphodiesterase inhibitors (pde3) 2012, november 13 [Available from: https://www.cvpharmacology.com/vasodilator/PDEI.

28.   Demuth DR. Gregory A. Petsko Dagmar Ringe Primers in Biology: Protein Structure and Function 2004 New Science Press, Ltd. 195 pages. Reproductive Toxicology. 2005;19(4):565-6.

29.   Homology Modeling: Methods and Protocols. Totowa, NJ: Humana Press, Totowa, NJ; 2012.

30.   The National Center for Biotechnology Information. Basic local alignment search tool 2020, Feburary 3 [Available from: https://blast.ncbi.nlm.nih.gov/Blast.cgi.

31.   Cheung PP, Yu L, Zhang H, Colman RW. Partial Characterization of the Active Site Human Platelet cAMP Phosphodiesterase, PDE3A, by Site-Directed Mutagenesis. Archives of Biochemistry and Biophysics. 1998;360(1):99-104.

32.   Bhattacharya A, Wunderlich Z, Monleon D, Tejero R, Montelione G. Assessing model accuracy using the homology modeling automatically software. Proteins. 2008;70(1):105-18.

33.   Laskowski RA, Macarthur MW, Moss DS, Thornton JM. PROCHECK : a program to check the stereochemical quality of protein structures. Journal of Applied Crystallography. 1993;26(2):283-91.

34.   Colovos C, Yeates TO. Verification of protein structures: Patterns of nonbonded atomic interactions. Protein Science. 1993;2(9):1511-9.

35.   Morris AL, Macarthur MW, Hutchinson EG, Thornton JM, Morris AL. Stereochemical quality of protein structure coordinates. Proteins. 1992;12(4):345-64.

36.   Pedersen TF, Thorbjørnsen ML, Klepstad P, Sunde K, Dale O. Therapeutic hypothermia--pharmacology and pathophysiology. Tidsskrift for den Norske laegeforening : tidsskrift for praktisk medicin, ny raekke. 2007;127(2):163.